Journal of Materials Chemistry A

Synthesis and Characterisation of Aqueous Miscible Organic-Layered Double Hydroxides

Journal:	*Journal of Materials Chemistry A*
Manuscript ID:	TA-ART-05-2014-002277.R1
Article Type:	Paper
Date Submitted by the Author:	10-Jul-2014

Complete List of Authors:
Chen, Chunping; Oxford University, Chemistry Research Laboratory
Yang, Miaosen; Oxford University, Chemistry Research Laboratory
Wang, Qiang; Beijing Forestry University, College of Environmental Science and Engineering
Buffet, Jean-Charles; Oxford University, Chemistry Research Laboratory
OHare, Dermot; Oxford University, Chemistry Research Laboratory

Journal of Materials Chemistry RSCPublishing

ARTICLE

Synthesis and Characterisation of Aqueous Miscible Organic-Layered Double Hydroxides

Cite this: DOI: 10.1039/xoxxoooooox

Chunping Chen,[†a] Miaosen Yang,[†a] Qiang Wang,*[b] Jean-Charles Buffet[a] and Dermot O'Hare*[a]

Received ooth January 2012,
Accepted ooth January 2012

DOI: 10.1039/xoxxoooooox

www.rsc.org/

We report the synthesis and characterisation of a new family of layered double hydroxides entitled Aqueous Miscible Organic Layered Double Hydroxide (AMO-LDH). AMO-LDHs have the chemical composition $[M^{z+}_{1-x}M'^{y+}_{x}(OH)_2]^{a+}(X^{n-})_{a/r}\bullet bH_2O\bullet c$(AMO-solvent) wherein M and M' are metal cations, z = 1 or 2; y = 3 or 4, $0 < x < 1$, b = 0 - 10, c = 0 - 10, X is an anion, r is 1 - 3 and $a = z(1-x)+xy-2$. The role of the AMO-solvents such as acetone (A) or methanol (M) in the LDH synthesis is discussed. The distinguishing features between AMO, and conventional or commercial LDHs are investigated using X-ray diffraction, infrared spectroscopy, electron microscopy, thermal analysis, adsorption and powder density studies. These experiments show that AMO-LDHs are highly dispersed and exhibit significantly higher surface areas and lower powder densities than conventional or commercially available LDHs. AMO-LDHs can exhibit N_2 BET surface areas in excess of 301 $m^2.g^{-1}$ compared to 13 $m^2.g^{-1}$ for the equivalent LDHs prepared by co-precipitation in water. The Zn_2Al-Borate LDH exhibits a pore volume of 2.15 $cc.g^{-1}$ which is 2534 times higher than the equivalent conventionally prepared LDH

1. Introduction

Layered double hydroxides (LDHs), also known as brucite-like 2D material, are regards as an important class of host-guest anionic clays which consists of positively charged metal hydroxide layer as host and negatively charged anionic interlayer as guest.[1] The most common LDH-based materials can be expressed by a general formula $[M^{2+}_{1-x}M^{3+}_{x}(OH)_2]^{x+}(A^{n-})_{x/n}\cdot mH_2O$, where M^{2+} and M^{3+} can be most divalent and trivalent metal cations, respectively; x is the metal ratio of M^{2+}/M^{3+}; A can be various anions.[2] Owing to their distinguishing features such as compositional flexibility, high anionic exchange ability and biocompatibility, LDHs have attracted considerable attention in the fields of catalyst, biomedicine, electrochemistry and environmental technologies.[3] However, the LDHs synthesised by conventional methods are often highly aggregated due to their high charge density and hydrophilicity. As a result, isolated LDH powders exhibit relatively low surface areas and unmodified forms cannot be dispersed in non-polar liquids, this imposes both severe limitations on their ability to be surface functionalised and their practical application. Therefore, in recent years many studies have been performed with the aiming of overcoming this limitation. To date, exfoliation methods and surfactant modification methods have been used to produce individual dispersions of LDH layers or thin nanosheets.[4] The organophilic anions which are used in these exchange processes modify the surface characteristics of LDH nanosheets and so reduce their interaction. However, this method normally requires the use of highly polar or even toxic solvents and a multi-step process. Furthermore, the isolated yields using such methods are relatively low and not practical for scale-up. Xu *et al.* has developed a simple and effective way to obtain individual LDH nanoparticles.[5] These nanoparticles may be dispersed in aqueous solution. However, we are interested in developing scalable methods for the dispersion of LDHs in non-polar hydrocarbon solvents, this would enable the use of LDHs to be realised in much wider fields of materials chemistry, catalysis and sorption.

Recently, we reported a simple and novel method, called the Aqueous Miscible Organic Solvent Treatment (AMOST) method, to obtain a new generation of Mg_3Al-CO_3, Zn_2Al-Borate and Mg_3Al-Borate LDHs which are highly dispersible in non-polar hydrocarbon solvents and exhibit high specific surface area (up to 458.6 $m^2.g^{-1}$).[6] In this method, the LDHs were synthesised by conventional co-precipitation method, but the final wet slurry was washed with an aqueous miscible organic (AMO) solvent. We found that the wet form of LDH slurry and 100 % aqueous miscible of solvent (e.g. acetone, methanol) are necessary to help improve the compatibility of LDHs with non-polar hydrocarbon solvents. AMO solvent treatment of LDHs can often lead to dispersion into thin nanosheets or exfoliation to even single layers. If we could apply this simple and cost-

effective method to all LDHs it would enable a new generation of LDH chemistry.

In this work, the AMOST method has been systematically investigated in order to develop a more and comprehensive understanding of the utility of the approach as a general method to prepare AMO-LDHs. Many new general distinguishing features of AMO-LDHs have been discovered by varying the composition of LDHs, the pH of synthesis process and by varying the AMO solvents. We also report a more complete study of their properties and characteristics. In particular, we are now able to define a generalised formula for the AMO-LDH family.

2. Experimental Part

2.1 Materials

$Mg(NO_3)_2{\cdot}6H_2O$ (AR), $Al(NO_3)_3{\cdot}9H_2O$ (AR), NaOH (AR), Na_2CO_3 (AR), $MgCl_2{\cdot}6H_2O$ (AR), $AlCl_3{\cdot}6H_2O$ (AR), NaCl (AR), $Fe(NO_3)_3{\cdot}9H_2O$ (AR), $MgSO_4{\cdot}7H_2O$ (AR), $Al_3(SO_4)_2{\cdot}16H_2O$ (AR), $Zn(NO_3)_2{\cdot}6H_2O$ (AR), $NaNO_3$ (AR) Na_2SO_4 (AR), H_3BO_3(AR), acetone (99.8%) methanol (99.8%), were purchased from Sigma-Aldrich Co. LLC. , and used without further purification. Deionized water (DI) was used throughout the experimental processes.

2.2 Experiments

General synthesis method for AMO-LDH

A metal precursor solution was added drop-wise into a base solution under rapid stirring. During this nucleation step, the pH value was constantly controlled by adding drop-wise a NaOH solution. After aging for 16 hours, the precipitate was washed with DI water until the pH was close to 7. Then, the obtained wet cake solid was dispersed into acetone followed by stirring for 1 - 2 hours. At the end of this dispersion step, the resultant solid was filtered and washed thoroughly with acetone. The final product was dried overnight in a vacuum oven at room temperature.

Specific examples of a conventional LDH (Mg_3Al-CO_3 LDH)

The metal precursor solution (50 mL) of 0.75 M $Mg(NO_3)_2{\cdot}6H_2O$ and 0.25 M $Al(NO_3)_3{\cdot}9H_2O$ was added drop-wise into the 50 mL of 0.5 M Na_2CO_3 base solution. The pH value was kept at *ca.* 10.0 by drop wise addition of a 4.0 M NaOH solution. This nucleation process takes 30 min. After aging for 16 h with stirring at room temperature, the mixture was filtered and washed with DI water until the pH was close to 7. The final product was dried overnight in a vacuum oven at room temperature. This sample was named as Mg_3Al-CO_3-10-W.

Specific examples of AMO-LDH (Mg_3Al-CO_3 LDH)

In the AMOST method, all the nucleation and aging steps are the same as those in the conventional method described above. The key difference is that in the AMOST method, the wet cake solid LDH obtained after washing with DI water is then further rinsed with acetone thoroughly. This acetone washed LDH is then redispersed in 200 mL acetone to give a slurry and stirred at room temperature for 1 - 2 h. The AMO-LDH is isolated by filtration. Finally, the product is dried overnight in a vacuum oven at room temperature. This sample is named as Mg_3Al-CO_3-10-A. If the AMO dispersion/washing solvent was methanol, this sample would be named as Mg_3Al-CO_3-10-M.

To the sake of clarity, the AMO-LDH samples described in this work was named as followed: $\mathbf{M_aM'_bM''_c}$**-X-P-S**, where *a*, *b* and *c* are the relative ratios of the metal cations in the layers; X is the intercalated anion, P is the pH of the synthesis solution; S is the washing solvent. For example, using the same synthesis condition and keeping the pH value at *ca.* 12.0, Mg_3Al-CO_3-12-W (C-LDH) and Mg_3Al-CO_3-12-A (AMO-LDH) would be synthesised by the conventional method and the AMOST method respectively.[3d] The full synthesis details of the AMO-LDHs containing different metal ratios or other metal cations can be found in the ESI. We use the shorthand term C-LDH to describe LDHs prepared by conventional LDHs precipitation techniques in water.

2.3 Powder X-ray diffraction

Powder X-ray diffraction (XRD) data were collected on a PANAnalytical X'Pert Pro diffractometer in reflection mode at 40 kV and 40 mA using Cu Kα radiation (α_1 = 1.54057 Å, α_2 = 1.54433 Å, weighted average = 1.54178 Å). Scans were recorded from $3^\circ \leq \theta \leq 70^\circ$ with varying scan speeds and slit sizes. Samples were mounted on stainless steel sample holders. The reflections at $2\theta = 43 - 44^\circ$ and 50° are produced by the XRD sample holder and can be disregarded.

2.4 Thermogravimetric analysis

Thermogravimetric analysis (TGA) measurements were collected using a Netzsch STA 409 PC instrument. TGA was used to determine the mass loss of a sample as a function of temperature. Approximately 20 mg of sample was heated in a corundum crucible between 30 °C and 600 °C at a heating rate of 10 °C min^{-1} under a stream of compressed N_2 flowing at 50 cm^3 min^{-1}. Differential thermogravimetric analysis (DTG) is obtained from the 1st derivative of TGA data.

2.5 Fourier Transform Infrared spectroscopy

Fourier Transform Infrared (FTIR) spectra were recorded on a Biorad FTS 6000 FTIR Spectrometer. It is equipped with a high performance DuraSamp1IR II diamond accessory of attenuated total reflection (ATR) mode in the range of 400-4000 cm^{-1} with 100 scans at 4 cm^{-1} resolution. The strong absorptions in the range 1667-2500 cm^{-1} are from the DuraSamp1IR II diamond surface.

2.6 Transmission Electron Microscopy

Transmission Electron Microscopy (TEM) analysis was performed on a JEOL 2100 microscope with an accelerating voltage of 200 kV. LDH nanoparticles were dispersed in ethanol with sonication and then casted onto copper grids coated with Formvar film.

2.7 Scanning Electron Microscopy

Scanning Electron Microscopy (SEM) analysis was performed on a Zeiss Supra 55 scanning electron microscope with an accelerating voltage of 20 kV. LDH powders were spread on carbon tape adhered to an SEM stage. Before imaging, the samples were coated with a thin platinum layer to prevent charging and to improve the image quality.

2.8 Energy-dispersive X-ray spectroscopy

Energy-dispersive X-ray Spectroscopy (EDX) was used to analyse the ratios of metal ions in the LDHs. LDH powders were spread on the carbon tape and coated with a thin platinum layer. The EDX data were collected from JSM-6610LV low vacuum SEM with an accelerating voltage of 20 kV.

2.9 Surface Area and Pore Size Analysis

Specific surface areas and pore size were analyzed using the Brunauer–Emmett–Teller (BET) method. The samples were measured from the N_2 adsorption and desorption isotherms at 77 K collected from a Quantachrome Autosorb-6 surface area and pore size analyzer. Before each measurement, LDH samples were first degassed overnight at 110 °C.

2.10 Density

The bulk density and tap density of AMO-LDHs and C-LDHs were measured by both standard test method (ASTM D7481-09) and GeoPyc 1360 Envelope Density Analyzer in Micrometric company. The procedure for standard test could be described as follows: The powder freely flowed into a graduated cylinder (10 mL) via the funnel. The cylinder with powder was tapped at an interval time of 30 s and fell at the constant height of 20 mm for each tap. The volume was measured before and after 300 taps. The Loose Bulk Density and Tap Density can be calculated by the equation (1) and (2), respectively.

$$\text{Loose Bulk Density} = \frac{m}{V_0} \quad (1)$$

$$\text{Tap Density} = \frac{m}{V_f} \quad (2)$$

Where m is the powder weight in the graduated cylinder, V_0 is the initial powder volume in the cylinder before tapping, V_f is the final powder volume in the cylinder after 300 taps.

3. Results and discussion

3.1 Physical properties of AMO-LDHs

Aqueous miscible organic-layered double hydroxide (AMO-LDHs) have been synthesised and their properties with respect to structure, morphology, surface, thermal and packed density have been studied. Some of the distinguishing features are listed in Table 1. Generally, AMO-LDHs exhibit lower packed powder density, higher surface area and lower decomposition temperature comparing to conventional layered double hydroxide (C-LDHs).

Table 1 Summary of the distinguishing features of AMO-LDHs compared to C-LDHs

Properties	Parameters	AMO-LDH	C-LDH	Change
Density	Loose Bulk Density[1] (g/mL)	0.1-0.18	0.29-0.95	38-84 %
	Tap Density[2] (g/mL)	0.16-0.26	0.39-1.2	41-82 %
	Carr's Index[3]	32-40	22-39	0-45 %
	Avg TAP Density[4] (g/mL)	0.35	0.49	39%
Surface	Surface Area (m^2/g)	61-301	1-148	34-11,100 %
	Pore Volume (cc/g)	0.305-2.15	0.00035-0.9	11-147,392 %
Thermal	T1[5](°C)	150-191	169-205	–6 - –9 (°C)
	T2[6](°C)	340-392	392-424	-7 - –84 (°C)

AMO-LDH is a LDH prepared using the AMOST method.
C-LDH is a LDH prepared using conventional co-precipitation techniques in water.
[1]Loose Bulk Density and [2]Tap Density were measured according to the Standard Test Method (ASTM D7481-09).
[3]Carr's Index was evaluated graphically by plotting (N/c) vs N according to the Kawakita Equation [7] $N/c = N/a + 1/ab$, where N is the number of taps, V represents the powder volume, V_0 is the initial powder volume before tapping, $c = (V_0 - V)/V_0$, a is the Carr's Index[7-8], b is the constant related to cohesiveness and shear strength, respectively.
[4]Avg TAP Density was measured by GeoPyc 1360 Envelope Density Analyser supplied by Micromeritics Ltd., http://www.micromeritics.com/pressroom/press-release-list/geopyc-1360-press-release.aspx
[5]T1 and [6]T2 are defined as the 1st and 2nd minima in 1st derivative of the TGA.

3.2 Structural properties

The structures of the obtained AMO-LDHs and C-LDHs were analysed using X-ray diffraction (Fig 1. and Fig. S1-S5). The results show that all AMO-LDHs exhibit the same XRD patterns as those of the conventional LDHs, indicating that the AMOST treatment does not affect the structure of the LDHs.

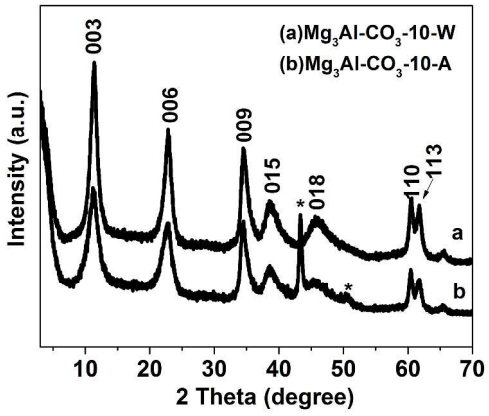

Fig. 1 XRD patterns for Mg_3Al-CO_3-10; (a) sample prepared by conventional co-precipitation method in water at pH 10 (b) sample prepared under identical synthesis conditions with the additional AMOST method treatment using acetone as the AMO-solvent. (*) are Bragg reflections from the Al sample holder.

For Mg_3Al-CO_3 LDH, acetone washed (AMO-LDH) and the conventional water washed (C-LDH), the expected 00*l* (*l* = 3, 6,

9) Bragg reflections were observed (Fig. 1). This is also observed for Mg_2Al-CO_3-10 LDH, Mg_3Al-CO_3-12, Mg_3Al-SO_4-10, Mg_3Al-CO_3-10-M, and Mg_3Al-SO_4-10-M (see Figs S1 - S5 respectively).

Similarly, the FTIR spectrum of Mg_3Al-CO_3-10 LDH shows that the structure of the LDH is unchanged using both synthesis methods (Fig. 2). Similar results were observed for Mg_3Al-CO_3-12, Mg_3Al-Cl-10, and Mg_3Al-NO_3-10 (see Figs. S6-S8 respectively).

Fig. 2 shows the FTIR spectrum for the AMO- and C-LDH. Both samples show the characteristic bands for the intercalated CO_3^{2-} (ν = 1368 cm^{-1}). Similar bands are observed when the LDHs were synthesised at pH = 12 (Fig. S6). When MgAl-NO_3-10 LDHs (acetone or water washed) were synthesised, the band corresponding to the anion was shown at ν = 1350 cm^{-1} (Fig. S8).

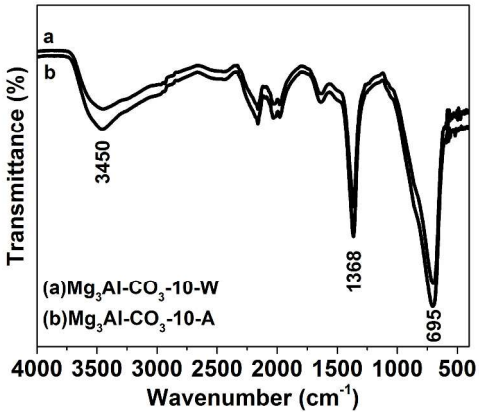

Fig. 2 FTIR spectrum of Mg_3Al-CO_3-10; (a) sample prepared by conventional co-precipitation method in water at pH 10 (b) sample prepared under identical synthesis conditions with the additional AMOST method treatment using acetone as the AMO-solvent.

3.3 Morphological study

The morphologies of LDHs were examined by TEM. Owing to the relatively high surface charge and hydrophilic nature of LDHs, we find that these particles or crystallites of conventionally synthesised C-LDHs are generally highly aggregated. The Mg_3Al-CO_3-10-W particles in Fig. 3a are stone-like. On the other hand, the TEM image in Fig. 3b for Mg_3Al-CO_3-10-A LDH sample shows a flower-type sample. The diameter of the flower is 120 - 250 nm. Similar results were observed for Mg_3Al-Cl-10, Mg_3Al-NO_3-10 and Mg_3Al-SO_4-10 (see Fig.S9-S11 respectively). The morphologies of the synthesised LDH powders were studied by SEM. The SEM of Mg_3Al-CO_3-10 is shown in Fig. 4. It can be easily observed that the Mg_3Al-CO_3-10-W platelet particles (Fig. 4a) are densely stacked on their *ab* face, resulting in the formation of hard stone-like clot (Fig. 4a inset) with a smooth surface. For Mg_3Al-CO_3-10-A (Fig. 4b), most particles are around 150 nm in size and stack in the c-direction to form loose flower-shape agglomerates, which have a more exposed surface. The same results were also found for other LDHs as shown in Fig. S12-S14. A commercial LDH (PURAL MG 62 HT) was also studied. The SEM image of a sample of PURAL MG 62 HT is shown in Fig. 4c, the sample is composed of agglomerates of around 25 μm in size.

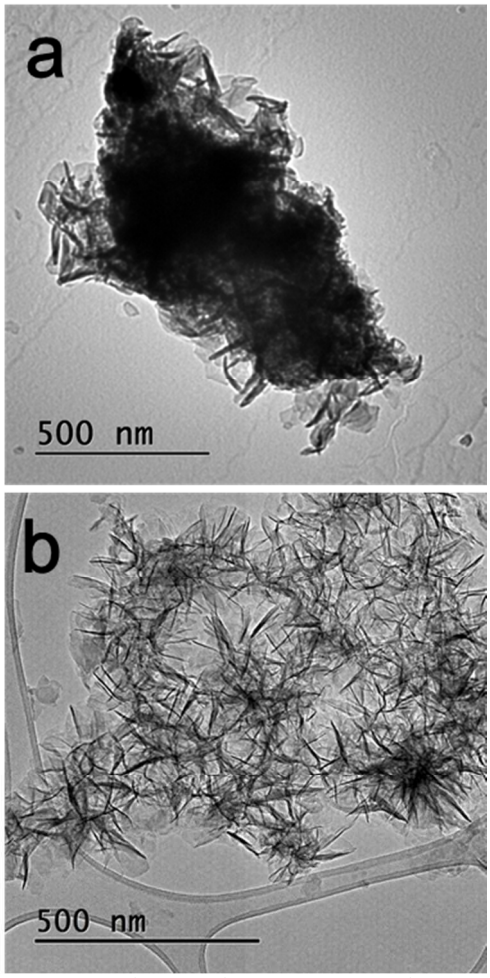

Fig. 3 TEM patterns for Mg_3Al-CO_3-10; (a) sample prepared by conventional co-precipitation method in water at pH 10 (b) sample prepared under identical synthesis conditions with the additional AMOST method treatment using acetone as the AMO-solvent.

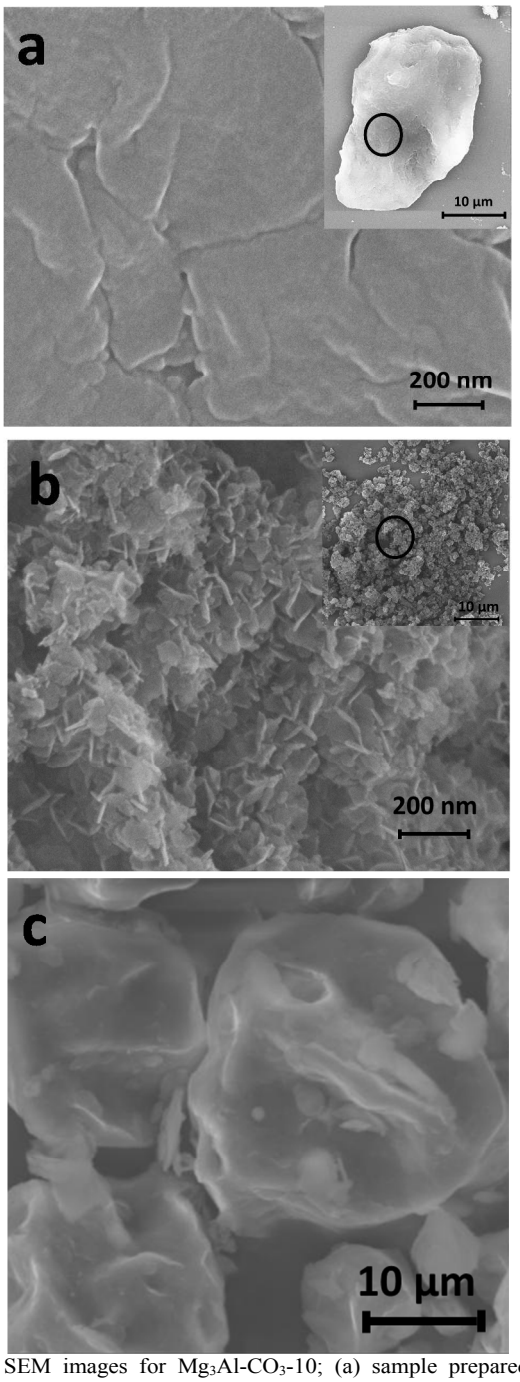

Fig. 4 SEM images for Mg_3Al-CO_3-10; (a) sample prepared by conventional co-precipitation method in water at pH 10 (b) sample prepared under identical synthesis conditions with the additional AMOST method treatment using acetone as the AMO-solvent (inset: the images at lower magnification); (c) a sample of a commercial hydrotalcite (PURAL MG 62 HT, from Sasol Ltd).

3.4 Thermal properties

The thermal properties of AMO-LDHs and C-LDHs were investigated using thermogravimetric analysis (TGA). As shown in Fig. 5a and Fig. S15a, the TGA curves of both AMO-LDH and C-LDHs exhibit the typical thermal decomposition behaviour of LDHs which has three weight losses in the range of 50 – 800 °C. By differentiation of the TGA curves, more detailed information regarding the subtlety of the thermal behaviour can be obtained as shown in DTG curves (Fig. 5a). It can be clearly found that all LDHs have two distinct events around 200 °C (noted as T1) and 400 °C (noted as T2). The weight loss below T1 is due to the desorption of physisorbed and intercalated solvents. After T1, the hydroxyl groups start to decompose and gradually transform the LDH structure. This reaches a maximum at around 400 °C (T2), and is normally ascribed to the partial decomposition of carbonate anions and complete dehydroxylation of the metal hydroxide layers.[9] However, the AMO-LDHs (either acetone or methanol) show lower decomposition temperatures compared to the C-LDHs. We believe this is a significant difference and is mainly due to the better dispersion of the AMO-LDH particles.

Table 2 highlights the changes in T1 and T2 for all the AMO-Mg_xAl-CO_3 LDHs (x = 2 or 3) compared with their equivalent C-LDH. For T1, the differences range from 6 to 19 °C lower for the AMO-LDHs compared to the corresponding C-LDHs. The change in T2 is more dramatic, with a decrease of 84 °C from 424 °C (for Mg_3Al-CO_3-10-W) to 340 °C (for Mg_3Al-CO_3-10-A).

Furthermore, we find an additional reproducible feature in the TGA of AMO-LDHs; this mass loss event is observed at low temperature (30 – 230 °C) as shown in Fig. 5b. We believe this mass loss is due to desorption of the AMO solvents from the AMO-LDHs, which have lower boiling points than H_2O. We find this feature in all AMO-LDHs such as Mg_3Al-NO_3-10-A, Mg_3Al-SO_4-10-A, $Mg_3Al_{0.5}Fe_{0.5}$-CO_3-10-A (see Fig. S15). This signature enable us do have define a new compositional formula for this family: $[M^{z+}_{1-x}M'^{y+}_{x}(OH)_2]^{a+}(X^{n-})_{a/r}\bullet bH_2O\bullet c$(AMO-solvent), which instantly distinguishes them from the normal general formula of LDH $[M^{z+}_{1-x}M'^{y+}_{x}(OH)_2]^{a+}(X^{n-})_{a/r}\bullet bH_2O$, wherein M and M' are metal cations, z = 1 or 2; y = 3 or 4, $0 < x < 1$, b = 0 - 10, c = 0 - 10, X is an anion, r is 1 to 3 and $a = z(1-x)+xy-2$. The details of the composition determined for each AMO-LDH and C-LDH are listed in Table 3 (Table S1). We find that AMO solvent content (c) in these samples is typically in the range of 0.04-0.18, which is 7 - 28 % in total solvent present (water and AMO-solvent). The AMO solvent is probably both bound to the surface of LDH and/or intercalated in the galleries of the LDH. Due to low content and small molecular size of these solvents (0.13 nm for methanol[10] and 0.44 nm for acetone [11]) compared to the main interlayer anions (such as CO_3^{2-}, 0.507 nm[12]), the XRD patterns do not resolve any difference between an AMO-LDH and a C-LDH.

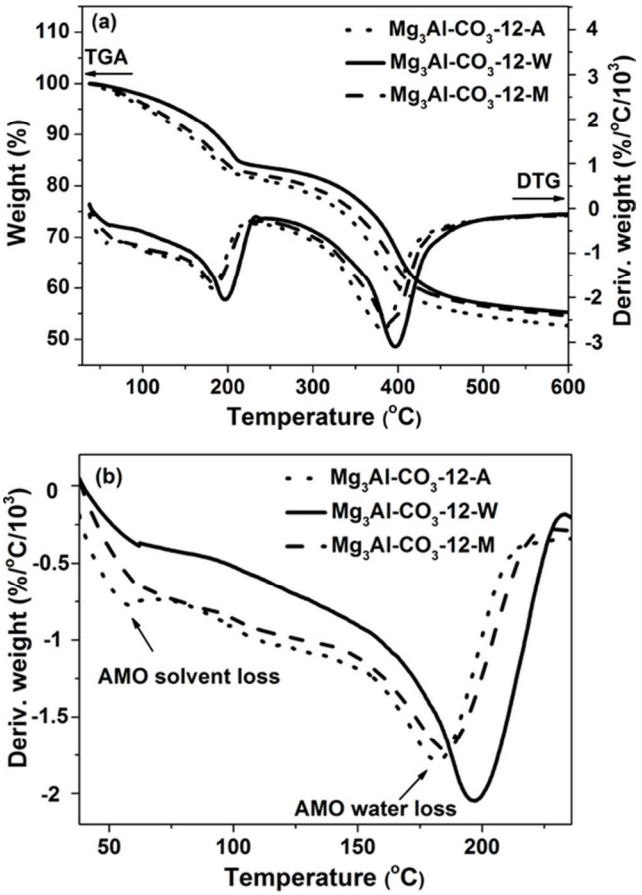

Fig. 5 TGA and DTG analysis of Mg_3Al-CO_3-12 LDHs (a) in the range of 30-600 °C; (b) in the range of 30-230 °C; Mg_3Al-CO_3-12-W prepared by a conventional co-precipitation method in water at pH 12. Mg_3Al-CO_3-12-A is prepared by identical conditions in water at pH 12 according to the AMOST method using acetone as the AMO-solvent.

3.5 Surface analysis

We were particularly interested in the surface area and pore volume of the AMO-LDHs. We recently reported that borate intercalated AMO-LDHs exhibit surface areas in excess of 301 m^2/g (Zn_2Al-Borate-8.3-A), compared to the N_2 BET surface area of 13 $m^2.g^{-1}$ for the equivalent Zn_2Al-Borate-8.3-W prepared in water.[6a] The pore volume of 2.15 $cc.g^{-1}$ for Zn_2Al-Borate-8.3-A which is 2534 times higher than the equivalent C-LDH sample. The theoretical maximum surface area for an AMO-LDHs could be as high as 850 $m^2.g^{-1}$ if we could achieve fully dispersed nanosheets. In order to determine if these high surface areas is a general phenomena we have extensively investigated the surface properties of a range of LDHs containing different cation and anion compositions. The surface properties are summarised in Table 4, the data clearly show that all AMO-LDHs have much higher surface areas than those of the equivalent C-LDHs. However, the percentage increase in the N_2 BET surface area each case varies from 34 - 26,200 % and the increase in the total pore volume is from 11 - 147,329 % comparing the C-LDH to the AMO-LDH. To date, MgAl-NO_3-10-A LDH has demonstrated the greatest increase of 11,167% in surface area, from 1.5 $m^2.g^{-1}$ to 169 $m^2.g^{-1}$. Furthermore, an increase of 9,581 % was observed in pore volume (0.0066 and 0.639 $cc.g^{-1}$ for C- and AMO-LDH, respectively).

The N_2 adsorption and desorption isotherms in Fig. 6 (see also Fig. S16 - S19) show that both of AMO-LDHs and C-LDHs exhibit type IV isotherm and H3 type hysteresis loop according to the IUPAC classification, indicating that all LDHs in this study are formed of plate-like particles with slit-shape pores. However, the N_2 desorption (Fig. 6a) is much slower compared to the C-LDHs (Fig. 6b), which is probably due to the presence of thinner AMO-LDH nanoplatelets and the presence of more mesopores generated during the AMOST treatment.

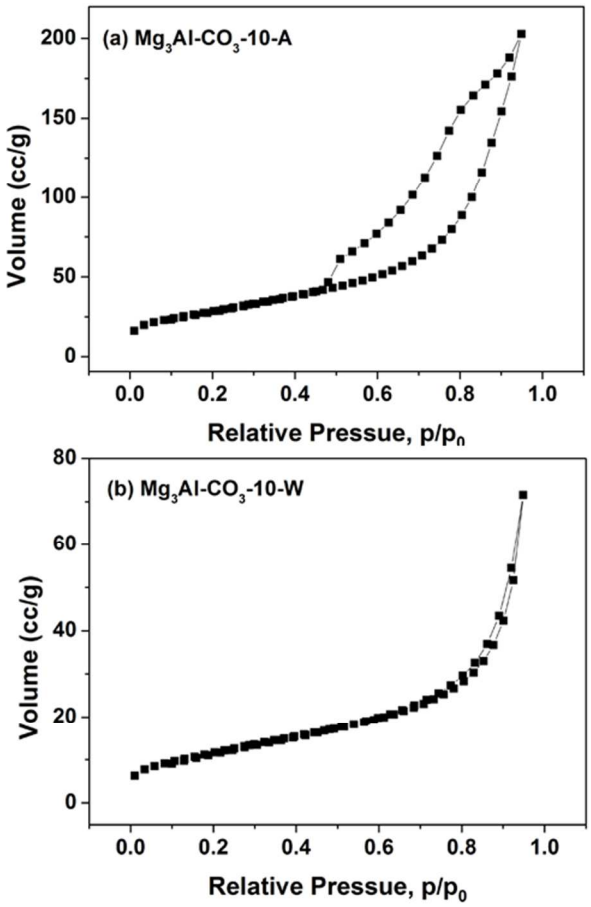

Fig. 6 N_2 BET adsorption isotherms for Mg_3Al-CO_3-10; (a) sample prepared under identical synthesis conditions with the additional AMOST method treatment using acetone as the AMO-solvent 10 (b) sample prepared by conventional co-precipitation method in water at pH 10.

3.6 Density

The powder density of the AMO-LDHs is one of the most striking initial observations upon initial synthesis and drying. We have investigated the powder density of the AMO-LDHs and compared the results with in the C-LDH and some commercial LDHs, using two measurement methods, a ASTM standard test method (ASTM D7481-09) and using a GeoPyc 1360 Envelope Density Analyzer). Fig. 7 shows the density curves of Mg_3Al-SO_4-10 with and without AMO solvent treatment using the ASTM D7481-09 method. The densities of both Mg_3Al-SO_4-10-A and Mg_3Al-SO_4-10-W increase with increasing tap number and reach a steady value after 100 taps. The loose bulk density can be obtained from the initial point and the last equilibrium point, respectively. It can be found that Mg_3Al-SO_4-10-A has a bulk powder density of 0.1 $g.mL^{-1}$ and a tap density of 0.16 $g.mL^{-1}$,

which is much lower than those of Mg_3Al-SO_4-10-W (0.41 $g.mL^{-1}$ and 0.63 $g.mL^{-1}$, respectively). The photos of both samples (1 g) after 300 taps clearly show that the AMO-LDH is much more loose compared to that using traditional method. This is ascribed to the delamination of LDH into thin nanosheets after AMO solvent treatment. Similar findings can also be obtained from other AMO-LDHs as shown in Fig. S20 - S23. To confirm the reliability of the obtained tap densities, measurements were also performed on a GeoPyc 1360 Envelope Density. Fig. S23 shows one example for Mg_3Al-CO_3 LDH.

Carr's Index, also called the Compressibility Index, was used to analyse the measured density results. Carr's Index can be obtained by plotting the *N/c* vs *N* according to the Kawakita Equation, $\frac{N}{c}=\frac{N}{a}+\frac{1}{ab}$, where *N* is the number of taps, $c = (V_0-V)/V_0$, *V* represents the powder volume, V_0 is the initial powder volume before tapping, *a* is the Carr's Index[7-8], *b* is the constant related to cohesiveness and shear strength. The data in Fig. 8 clearly shows that the Carr's Index (1/slope) of Mg_3Al-SO_4-10-A is higher than that of Mg_3Al-SO_4-10-W, indicating the AMO-LDHs has a higher compressibility compared to C-LDH.

A summary of the density studies data for all the AMO-LDHs, C-LDHs and commercial LDHs are listed in Tables 5,6. We find that all the AMO-LDHs show lower densities (both loose bulk density and tap density) between 38 – 82 % compared to the equivalent C-LDHs. Compared to commercial LDHs, the AMO-LDH densities are 68 – 70 % less than for example PURAL™ MG 62. In addition, the Carr's Indexes of AMO-LDHs are generally higher (0 – 45 %) than those of C-LDHs and commercial LDHs.

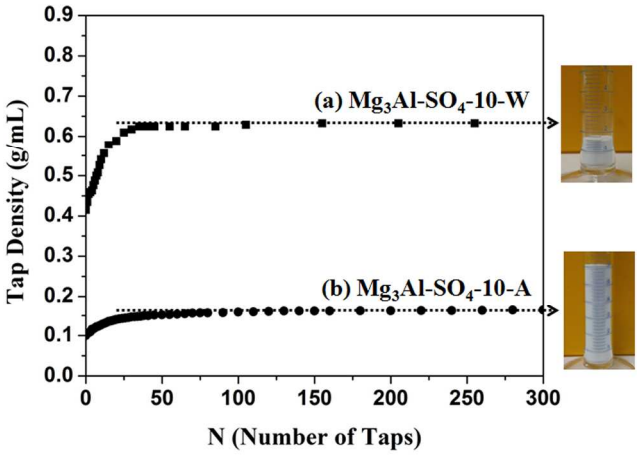

Fig. 7 Bulk powder tap density measurement for Mg_3Al-SO_4-10 LDH; (a) sample prepared by a conventional co-precipitation method in water at pH 10 and (b) AMOST method using the AMO-solvent acetone (insets are digital photos with 1g of samples after 300 taps).

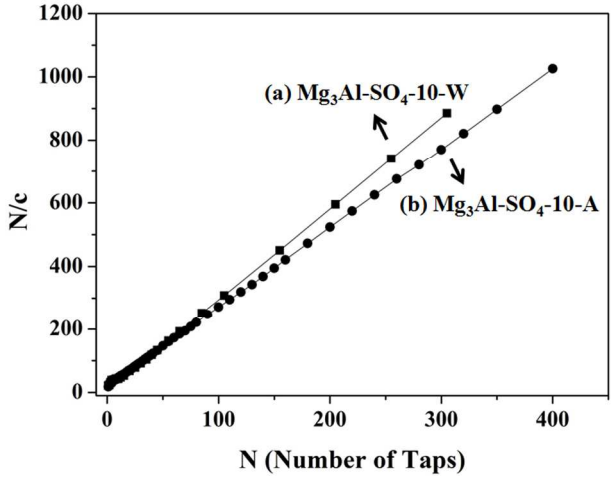

Fig. 8 Carr's index curves of Mg_3Al-SO_4-10 LDHs; (a) sample prepared by a conventional co-precipitation method in water at pH 10 and (b) AMOST method using the AMO-solvent acetone.

Table 2 Summary of the thermal properties of AMO-LDHs and C-LDHs

LDH	T1[3] (°C)			T2[4] (°C)		
	AMO-LDH-A[1]	C-LDH[2]	Change	AMO-LDH-A[1]	C-LDH[2]	Change
Mg_3Al-CO_3-12	187	205	–18	382	399	–17
Mg_3Al-CO_3-10	150	169	–19	340	424	–84
Mg_2Al-CO_3-10	181	187	–6	347	392	–45
Mg_3Al-CO_3-12[M]	191	205	–14	392	399	–7

[1]AMO-LDH-S is the LDH with the formula of $[M^{z+}_{1-x}M'^{y+}_{x}(OH)_2]^{a+}(X^{n-})_{a/r}\bullet bH_2O\bullet c$(AMO-solvent) (1) wherein M and M' are metal cations, z = 1 or 2; y = 3 or 4, $0<x<1$, b =0-10, c = 0-10, X is an anion, r = 1 - 3 and $a = z(1–x)+xy–2$, AMO-solvent (A = Acetone, M = Methanol)

[2]C-LDH is an LDH with the formula $[M^{z+}_{1-x}M'^{y+}_{x}(OH)_2]^{a+}(X^{n-})_{a/r}\bullet bH_2O$ wherein M and M' are metal cations, z = 1 or 2; y = 3 or 4, $0< x <1$, b = 0-10, c = 0-10, X is an anion, r = 1 - 3 and $a = z(1–x)+xy–2$.

[3]T1 and [4]T2 are defined as the 1st and 2nd minima in 1st differential of the TGA, respectively (i.e. when 2nd derivative of the TGA is zero)

Table 3 Summary of the chemical formula of the AMO-LDHs and C-LDHs using the thermal analysis data

LDH	Formula of AMO-LDH-A[1]	Formula of C-LDH[2]
Mg_3Al-CO_3 -10	$Mg_{0.75}Al_{0.25}(OH)_2(CO_3)_{0.125}$ •0.34(H_2O) •0.04(Acetone)	$Mg_{0.75}Al_{0.25}(OH)_{1.96}(CO_3)_{0.115}$•0.41($H_2O$)
Mg_2Al-CO_3 -10	$Mg_{0.75}Al_{0.35}(OH)_{2.2}(CO_3)_{0.175}$•0.59($H_2O$)•0.18(acetone)	$Mg_{0.75}Al_{0.35}(OH)_{2.2}(CO_3)_{0.175}$•1.05($H_2O$)
Mg_3Al-CO_3-12	$Mg_{0.75}Al_{0.22}(OH)_{1.94}(CO_3)_{0.11}$•0.43($H_2O$)•0.11(Acetone)	$Mg_{0.75}Al_{0.24}(OH)_{1.98}(CO_3)_{0.12}$•0.7($H_2O$)
$Mg_3Al_{0.5}Fe_{0.5}$-NO_3-10	$Mg_{0.75}Al_{0.12}Fe_{0.11}(OH)_{1.96}(CO_3)_{0.115}$•0.5($H_2O$)•0.06(acetone)	$Mg_{0.75}Al_{0.12}Fe_{0.13}(OH)_2(CO_3)_{0.125}$•0.74($H_2O$)
Mg_3Al-SO_4-10	$Mg_{0.75}Al_{0.66}(OH)_{2.82}(SO_4)_{0.33}$•0.71($H_2O$)•0.17(acetone)	$Mg_{0.75}Al_{0.45}(OH)_{2.4}(SO_4)_{0.225}$•0.77($H_2O$)
Mg_3Al-NO_3-10	$Mg_{0.75}Al_{0.25}(OH)_{1.96}(NO_3)_{0.23}$•0.38($H_2O$)•0.12(acetone)	$Mg_{0.75}Al_{0.25}(OH)_2(NO_3)_{0.25}$•0.57($H_2O$)
Mg_3Al-Cl-10	$Mg_{0.75}Al_{0.23}(OH)_{1.96}(Cl)_{0.23}$•0.46($H_2O$) •0.04(acetone)	$Mg_{0.75}Al_{0.22}(OH)_{1.94}(Cl)_{0.22}$•0.58($H_2O$)
Mg_3Al-CO_3 -12	$Mg_{0.75}Al_{0.24}(OH)_{1.98}(CO_3)_{0.12}$•0.43($H_2O$)•0.11(methanol)	$Mg_{0.75}Al_{0.24}(OH)_{1.98}(CO_3)_{0.12}$•0.7($H_2O$)

[1]AMO-LDH-S is the LDH with the formula of $[M^{z+}_{1-x}M'^{y+}_x(OH)_2]^{a+}(X^{n-})_{a/r}$•$b$$H_2O$•$c$(AMO-solvent), wherein M and M' are metal cations, z = 1 or 2; y = 3 or 4, 0< x <1, b = 0-10, c = 0-10, X is an anion, r = 1- 3 and $a = z(1–x)+xy–2$. AMO-solvent (A = Acetone, M = Methanol)
[2]C-LDH is an LDH with the formula $[M^{z+}_{1-x}M'^{y+}_x(OH)_2]^{a+}(X^{n-})_{a/r}$•$b$$H_2O$ (2) wherein M and M' are metal cations, z = 1 or 2; y = 3 or 4, 0 < x < 1, b = 0-10, c = 0-10, X is an anion, r = 1 to 3 and $a = z(1–x)+xy–2$.

Table 4 Summary of the surface properties of AMO-LDHs and C-LDHs

LDH	Surface Area ($m^2.g^{-1}$)			Pore Volume ($cc.g^{-1}$)		
	AMO-LDH-A[1]	C-LDH[2]	Change(%)	AMO-LDH-A[1]	C-LDH[2]	Change(%)
Mg_3Al-CO_3 -10	212	43	393	0.63	0.11	472
Mg_2Al-CO_3 -10	199	148	34	1	0.9	11
Mg_3Al-CO_3-12	148	41	261	0.405	0.13	222
$Mg_3Al_{0.5}Fe_{0.5}$-NO_3-10	128	91	41	1.1	0.68	62
Zn_2Al-Borate-8.3	301	13	2,215	2.15	0.0816	2,534
Mg_3Al-Borate-9	263	1	26,200	0.516	0.00035	147,329
Mg_3Al-SO_4-10	101	14	621	0.305	0.012	2442
Mg_3Al-NO_3-10	169	1.5	11,167	0.639	0.0066	9,581
Mg_3Al-Cl-10	64	1	6,300	0.319	0.0031	10,190
Zn_3Al-NO_3-8.3	61	1	6,000	0.37	0.016	2,212
Mg_3Al-CO_3 -12[M]	157	43	217	0.94	0.11	755

[1]AMO-LDH-S is the LDH with the formula of $[M^{z+}_{1-x}M'^{y+}_x(OH)_2]^{a+}(X^{n-})_{a/r}$•$b$$H_2O$•$c$(AMO-solvent) wherein M and M' are metal cations, z = 1 or 2; y = 3 or 4, 0 < x < 1, b = 0-10, c = 0-10, X is an anion, r is 1 to 3 and $a = z(1–x)+xy–2$. AMO-solvent (A = Acetone, M = Methanol)
[2]C-LDH is an LDH with the formula $[M^{z+}_{1-x}M'^{y+}_x(OH)_2]^{a+}(X^{n-})_{a/r}$•$b$$H_2O$ (2) wherein M and M' are metal cations, z = 1 or 2; y = 3 or 4, 0 < x < 1, b = 0-10, c = 0-10, X is an anion, r = 1 - 3 and $a = z(1–x)+xy–2$.

Table 5. Summary of the powder density of various AMO-LDHs and C-LDHs.

LDH	Loose Bulk Density (g/ml)			Tap Density ($g.ml^{-1}$)			Carr's Index		
	AMO-LDH-A[1]	C-LDH[2]	Change(%)	AMO-LDH-A[1]	C-LDH[2]	Change(%)	AMO-LDH-A[1]	C-LDH[2]	Change(%)
Mg_3Al-SO_4-10	0.1	0.41	76	0.16	0.63	75	40	35	14
Mg_3Al-NO_3-10	0.15	0.95	84	0.22	1.2	82	32	22	45
Mg_3Al-Cl-10	0.18	0.29	38	0.26	0.44	41	35	35	0

[1]AMO-LDH-A and AMO-LDH-M are the LDHs with the formula of $[M^{z+}_{1-x}M'^{y+}_x(OH)_2]^{a+}(X^{n-})_{a/r}$•$b$$H_2O$•$c$(AMO-solvent), wherein M and M' are metal cations, z = 1 or 2; y = 3 or 4, 0 < x < 1, b = 0-10, c = 0-10, X is an anion, r is 1 to 3, $a = z(1–x)+xy–2$, AMO-solvent (A=Acetone, M=Methanol).
[2]C-LDH is the LDHs with the formula of $[M^{z+}_{1-x}M'^{y+}_x(OH)_2]^{a+}(X^{n-})_{a/r}$•$b$$H_2O$ wherein M and M' are metal cations, z = 1 or 2; y = 3 or 4, 0 < x < 1, b = 0-10, c = 0-10, X is an anion, r = 1 - 3 and $a = z(1–x)+xy–2$.

Table 6. Summary of the powder density of various AMO-LDHs and a commercial LDH.

LDH	Loose Bulk Density ($g.ml^{-1}$)			Tap Density ($g.ml^{-1}$)			Carr's Index		
	AMO-LDH-A[1]	MG[2] 62	Change(%)	AMO-LDH-A[1]	MG[2] 62	Change(%)	AMO-LDH-A[1]	MG[2] 62	Change(%)
Mg_3Al-CO_3-10	0.14	0.46	70	0.2	0.64	68	35	29	20

[1]AMO-LDH-A and AMO-LDH-M are the LDHs with the formula of $[M^{z+}_{1-x}M'^{y+}_x(OH)_2]^{a+}(X^{n-})_{a/r}$•$b$$H_2O$•$c$(AMO-solvent), wherein M and M' are metal cations, z = 1 or 2; y = 3 or 4, 0 < x < 1, b = 0-10, c = 0-10, X is an anion, r is 1 - 3, $a = z(1–x)+xy–2$, AMO-solvent (A=Acetone, M=Methanol).
0-10, X is an anion, r = 1 - 3 and $a = z(1–x)+xy–2$.
[2]MG 62 is the commercial hydrotalcite, PURAL MG 62 HT, from Sasol Ltd.

4. Summary and Conclusions

We report the synthesis and characterisation of a new family of layered double hydroxides entitled Aqueous Miscible Organic Layered Double Hydroxide (AMO-LDH). We have determined that AMO-LDHs have the unique chemical composition $[M^{z+}_{1-x}M'^{y+}_x(OH)_2]^{a+}(X^{n-})_{a/r}$•$b$$H_2O$•$c$(AMO-solvent). Although the LDHs that are synthesised using the AMOST and conventional methods possess the same structural properties as shown by XRD. The AMO-LDHs possess new physical properties; they

have significantly higher surface areas, pore volumes, together with lower density and higher compressibility than both conventional and commercial LDHs. The role of the AMO-solvent (eg acetone and methanol) is the subject to further theoretical and experiment investigation. Our current thoughts (Fig. 9) are that the AMO solvent replaces the surface bound water from the surface of primary LDH particles and so rendering them hydrophobic rather than hydrophilic. These hydrophobic particles would then have a much-diminished driving force for aggregation to dense agglomerates.

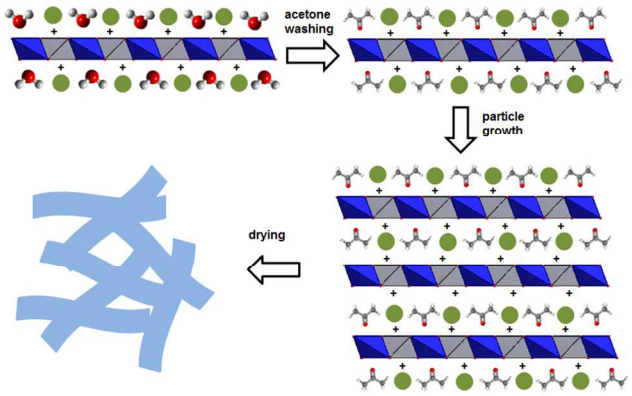

Fig. 9 The proposed mechanism for the formation of AMO-LDHs using acetone treatment.

We are already finding that AMO-LDHs are good candidates for wide variety of applications such as additives to polymers, sorbents and catalyst supports. These results will be published in due course.

Acknowledgements

This work is supported SCG Chemicals, Bangkok, Thailand and by the Fundamental Research Funds for the Central Universities (TD-JC-2013-3), the Program for New Century Excellent Talents in University (NCET-12-0787).

Notes and references

[†] Chunping Chen and Miaosen Yang contribute equally to the project and are to be considered co-first authors.

[a] Chemistry Research Laboratory, Department of Chemistry, University of Oxford, 12 Mansfield Road, Oxford, OX1 3TA, UK. E-mail: dermot.ohare@chem.ox.ac.uk; Tel: +44 (0)1865 272686

[b] College of Environmental Science and Engineering, Beijing Forestry University, 35 Qinghua East Road, Haidian District, Beijing 100083, China. E-mail: qiang.wang.ox@gmail.com; qiangwang@bifu.edu.cn; Tel: 86-13699130626.

Electronic Supplementary Information (ESI) available: [Figures including X-ray diffraction patterns, Fourier transform infrared spectroscopy, transmission electron miscroscopy, BET analysis, thermogravimetric analysis and density studies]. See DOI: 10.1039/b000000x/

[1] a) X. Duan and D. G. Evans, *Layered double hydroxides*, Springer Verlag, **2006**, p; b) V. Rives, *layered double hydroxides: present and future*, Nova Science Publishers, **2001**, p; c) F. Cavani, F. Trifiro and A. Vaccari, *Catalysis today* **1991**, *11*, 173-301.

[2] *Zeta Potential of Colloids in Water and Waste Water*, American Society for Testing and Materials, **1985** p.

[3] a) Y. Zhao, B. Li, Q. Wang, W. Gao, C. J. Wang, M. Wei, D. G. Evans, X. Duan and D. O'Hare, *Chemical Science* **2014**, *5*, 951-958; b) C. Chen, L. K. Yee, H. Gong, Y. Zhang and R. Xu, *Nanoscale* **2013**, *5*, 4314-4320; c) Z. Gao, J. Wang, Z. Li, W. Yang, B. Wang, M. Hou, Y. He, Q. Liu, T. Mann and P. Yang, *Chemistry of Materials* **2011**, *23*, 3509-3516; d) Q. Wang, Y. Gao, J. Luo, Z. Zhong, A. Borgna, Z. Guo and D. O'Hare, *RSC Advances* **2013**, *3*, 3414-3420; e) C. Chen, P. Gunawan, X. W. D. Lou and R. Xu, *Advanced Functional Materials* **2012**, *22*, 780-787; f) J. H. Choy, S. Y. Kwak, J. S. Park, Y. J. Jeong and J. Portier, *Journal of the American Chemical Society* **1999**, *121*, 1399-1400; g) M. Yang, J. Liu, Z. Chang, G. R. Williams, D. O'Hare, X. Zheng, X. Sun and X. Duan, *Journal of Materials Chemistry* **2011**, *21*, 14741-14746.

[4] a) Q. Wang and D. O'Hare, *Chemical reviews* **2012**, *112*, 4124-4155; b) L. Li, Y. Feng, Y. Li, W. Zhao and J. Shi, *Angewandte Chemie International Edition* **2009**, *48*, 5888-5892; c) M. Adachi-Pagano, C. Forano and J.-P. Besse, *Chemical Communications* **2000**, 91-92.

[5] a) Z. P. Xu, G. Stevenson, C.-Q. Lu and G. Q. Lu, *The Journal of Physical Chemistry B* **2006**, *110*, 16923-16929; b) Z. P. Xu, G. S. Stevenson, C.-Q. Lu, G. Q. Lu, P. F. Bartlett and P. P. Gray, *Journal of the American Chemical Society* **2006**, *128*, 36-37.

[6] a) Q. Wang and D. O'Hare, *Chemical Communications* **2013**, *49*, 6301-6303; b) N. P. Funnell, Q. Wang, L. Connor, M. G. Tucker, D. O'Hare and A. L. Goodwin, *Nanoscale* **2014**, *6*, 8032-8036.

[7] K. Kawakita and K.-H. Lüdde, *Powder technology* **1971**, *4*, 61-68.

[8] P. Denny, *Powder Technology* **2002**, *127*, 162-172.

[9] W. Yang, Y. Kim, P. K. Liu, M. Sahimi and T. T. Tsotsis, *Chemical Engineering Science* **2002**, *57*, 2945-2953.

[10] Y.-S. Park and Y. Yamazaki, *Polymer Bulletin* **2005**, *53*, 181-192.

[11] H. Huang, J. Zhou, S. Chen, L. Zeng and Y. Huang, *Sensors and Actuators B: Chemical* **2004**, *101*, 316-321.

[12] Z. Xu and H. Zeng, *The Journal of Physical Chemistry B* **2001**, *105*, 1743-1749.

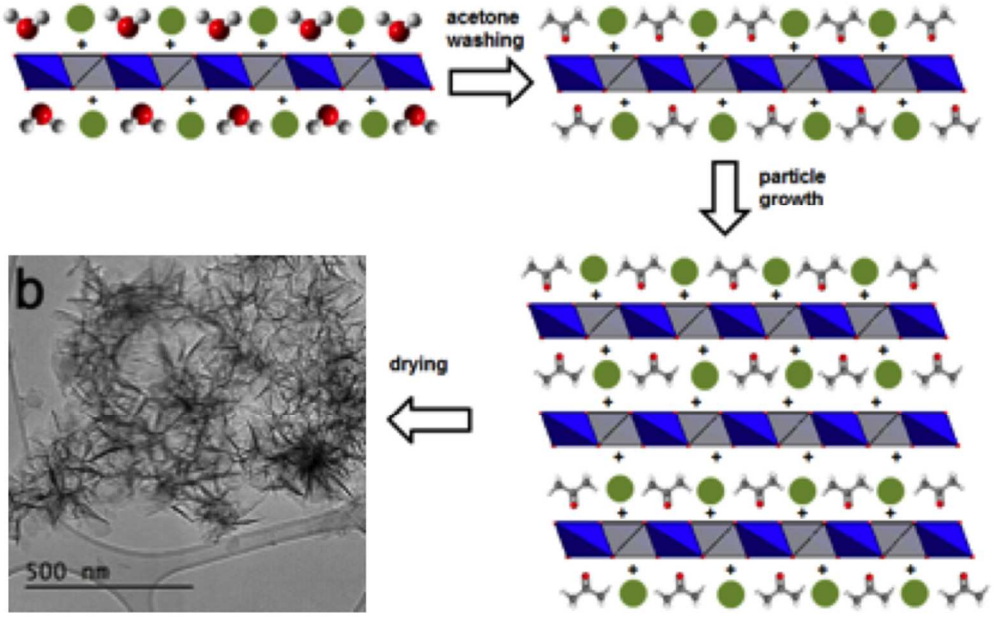

87x54mm (300 x 300 DPI)